Application of a load-bearing passive and active vibration isolation system in hydraulic drives

Oliver Unruh, Thomas Haase, Martin Pohl

Institute of composite structures and adpative systems, German Aerospace Center (DLR), Lilienthapltaz 7, 38108 Braunschweig, Germany

E-mail: oliver.unruh@dlr.de, thomas.haase@dlr.de, martin.pohl@dlr.de

Abstract. Hydraulic drives are widely used in many engineering applications due to their high power to weight ratio. The high power output of the hydraulic drives produces high static and dynamic reaction forces and moments which must be carried by the mounts and the surrounding structure. A drawback of hydraulic drives based on rotating pistons consists in multi-tonal disturbances which propagate through the mounts and the load bearing structure and produce structure borne sound at the surrounding structures and cavities. One possible approach to overcome this drawback is to use an optimised mounting, which combines vibration isolation in the main disturbance direction with the capability to carry the reaction forces and moments.

This paper presents an experimental study, which addresses the vibration isolation performance of an optimised mounting. A dummy hydraulic drive is attached to a generic surrounding structure with optimised mounting and excited by multiple shakers. In order to improve the performance of the passive vibration isolation system, piezoelectric transducers are applied on the mounting and integrated into a feed-forward control loop. It is shown that the optimised mounting of the hydraulic drive decreases the vibration transmission to the surrounding structure by 8 dB. The presented study also reveals that the use of the active control system leads to a further decrease of vibration transmission of up to 14 dB and also allows an improvement of the vibration isolation in an additional degree of freedom and higher harmonic frequencies.

1. Introduction

Due to their high power to weight ratio, hydraulic drives and actuators are widely used in many engineering applications. Especially in aerospace, where requirements regarding weight, power output and installation space are very strict, hydraulic drives and actuators became a primary components of flight control systems. Hydraulic actuators which produce axial loads are usually deflecting surfaces of the primary control system e.g. elevator, aileron and rudder. The secondary control system, which includes e.g. leading and trailing edge high-lift devices is powered by hydraulic drives with high torque output. In the high-lift control system the so-called power control units (PCU) are used in order to drive slats on the leading edge and flaps on the trailing edge. They are located under the passenger deck and connected by a complex system of shafts, gearboxes and track actuators which initially drive the high-lift devices. An overview of the secondary control system including slat and flap PCU is shown for the Airbus A320 aircraft in Figure 1 [1].

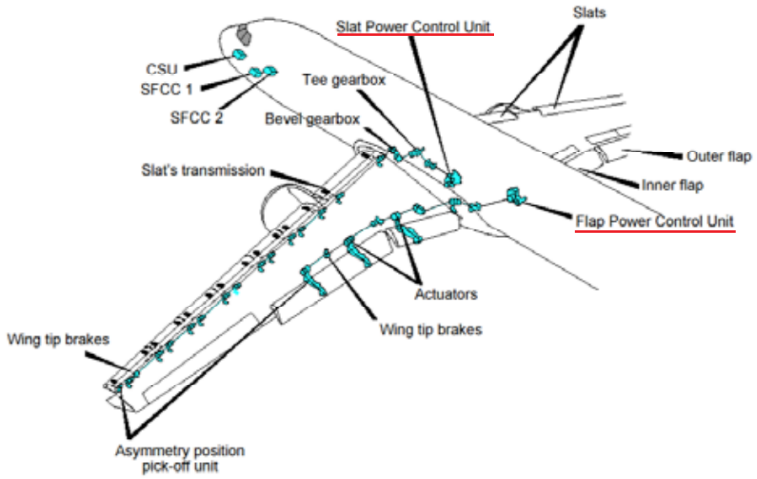

Figure 1: High-lift control system of the A320 aircraft [1]

Depending on the type of the aircraft, the PCU includes a redundant combination of two hydraulic drives or one hydraulic and one electric drive and can reach approx. 50 kg of weight. The PCU produces very high torque of more than 1500 Nm in maximum, which is required to drive the high-lift devices at the whole leading or trailing edge, even against aerodynamic loads at higher speeds. In order to transfer this high static and dynamic loads, the PCU is attached at the points where the structural stiffness of the fuselage structure is high.

During the operation the cylindrical pistons of the hydraulic drive are sequentially filled with high pressure hydraulic fluid. This process is the main source of vibration which is induced by a hydraulic drive. The fundamental frequency of disturbance results from the number of pistons and the rotational frequency of the hydraulic drive [2]. Additionally higher harmonic frequencies are present in the dynamic response of the PCU, which correspond to multiples of the fundamental frequency.

In general, the vibration of the PCU is transmitted into the passenger cabin by three transfer paths [3]. The first transfer path is the hydraulic fluid noise that propagates through pipes on the low and high pressure side of the PCU. Hydraulic pipes are connected to the fuselage structure by attachments, where the fluid noise converts to structure borne sound and propagates to the passenger cabin. The second transfer path corresponds directly to structure borne sound which is transmitted through the mounting of the PCU into the fuselage structure. Finally the third transfer path is related to the airborne noise which is radiated directly by the PCU body. Due to the fact, that the PCU is usually located in the system compartment which is isolated from the cabin, the airborne noise probably has a minor importance.

In current generation aircrafts the PCU only operates during take-off and landing, where the multi-tonal disturbances are not relevant for passenger comfort. In contrast, new generation aircrafts also use high-lift devices in cruise flight for the optimisation of aerodynamics and load distribution [4]. Due to the fact that especially on long-haul flights the cruise phase is used for resting, the sudden operation of the PCU can lead to waking reactions and reduce passenger comfort. One of the possible solutions consists in the reduction of the structure borne sound, which is transmitted through the PCU mounting into the fuselage structure, by means of passive and active vibration isolation. The passive isolation of vibrating devices such as automotive engines is well known from the literature [5]. The basic principle of passive isolation is the reduction of the dynamic stiffness of mounts with the use of e.g. hydraulic [6] or elastic

elements [7]. The main idea behind active vibration isolation is the application of counteracting dynamic forces in order to suppress the transmission of disturbances [8], [9]. The presented study addresses these topics and it is primarily focused on the experimental realisation of the vibration isolation, which has the capability to carry the mentioned reaction torque and enables a simple integration into the existing operational environment.

In the first part of the paper the dynamic behaviour of the PCU is analysed using data that have been captured in the aircraft during ground-tests. This analysis reveals critical frequencies and degrees of freedom (DOFs) which must be addressed by the vibration isolation system. In the next step a simplified demonstrator of the PCU with representative dynamic behaviour is presented. This demonstrator allows the characterisation of the vibration transmission through the currently used and the improved passive and active PCU mounting. In the main part of the paper the improved PCU mounting is presented and characterised in comparison to the reference mounting regarding vibration isolation performance. Furthermore it is shown that an active control system based on piezoelectric transducers and feed-forward control algorithm is able to improve the performance of the passive mounting and even extends the isolation to additional DOFs and higher harmonic frequencies.

2. Dynamic characterisation of the PCU

In order to identify critical frequencies and DOFs of the PCU motion, ground vibration tests are performed on the aircraft. For reasons of confidentiality the absolute values such as peak torque, sound pressure levels etc. cannot be given in this paper. Figure 2 exemplarily shows the PCU with the reference mounting, the drive shaft and the coordinate system which is used in this paper. In the ground test the PCU is equipped with three triaxial accelerometers, which acquire time data during the PCU operation (actuation of the trailing edge high-lift devices). This time data is required for the calculation of the rigid body motion of the PCU including three translational and three rotational DOFs.

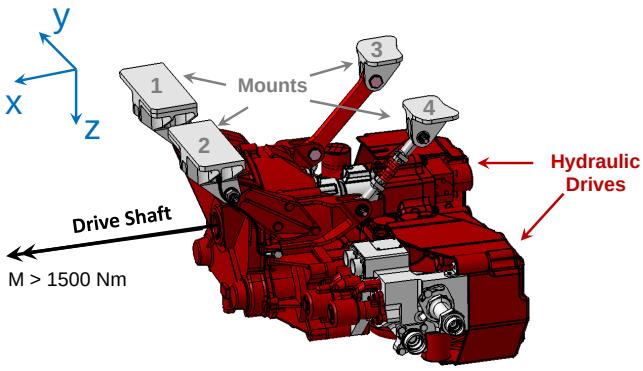

Figure 2: Investigated power control unit (PCU) with the reference mounting

In the first step of the dynamic characterisation of the PCU the time data is transferred into the frequency domain by the fast fourier transform (FFT). The spectrum of the structural acceleration, averaged over all sensor channels is shown in Figure 3(a). It can be noticed that the dynamic response of the PCU is dominated by the fundamental tone of 884 Hz and its higher harmonics. The fundamental frequency results from the rotational frequency multiplied with the number of pistons.

In order to identify tones that can disturb passengers, additional microphones are installed in the aircraft cabin. Figure 3(b) shows the averaged sound pressure levels that are measured

in the aircraft cabin during the PCU operation on ground. The acoustics in the cabin is also dominated by the fundamental frequency and its higher harmonics. It is important to notice that due to the lower transmission loss of the fuselage structure at lower frequencies the fundamental 884 Hz tone is approximately 6 dB higher than its higher harmonics. This means that passive and active isolation system must primarily address the disturbance at 884 Hz.

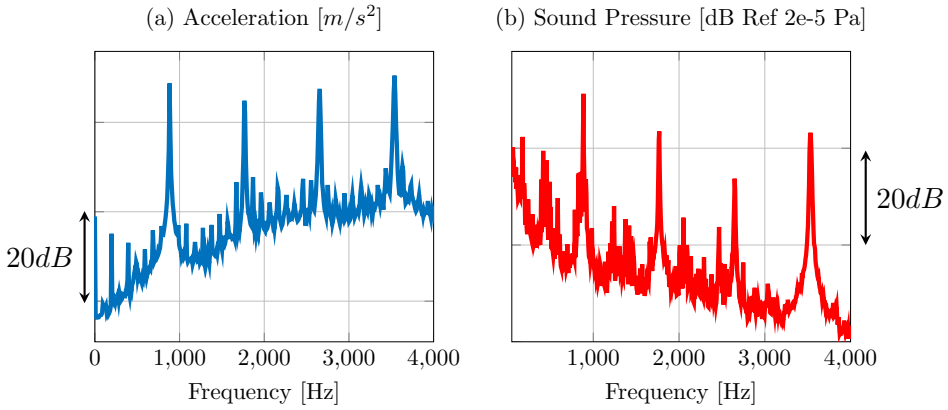

Figure 3: Accleleration of the PCU and sound pressure levels measured in the cabin

After the identification of the critical disturbance frequency the rigid body motion of the PCU is considered using the data measured by three triaxial accelerometers. Using the analysis of the rigid body motion presented in [10] the frequency dependant complex motion vector can be estimated. This vector includes six complex numbers which represent three translational and three rotational DOFs. Each complex number contains amplitude and phase of the corresponding DOF of the rigid body motion. Figure 4 shows the elements of the rigid body motion vector in the complex plane for the fundamental frequency of 884 Hz.

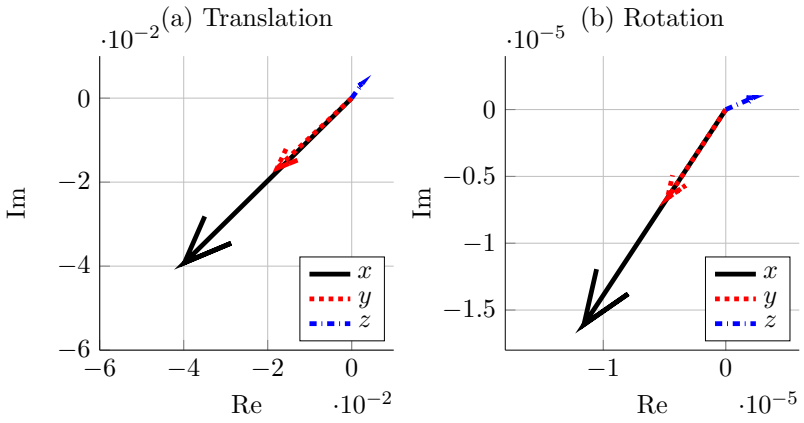

Figure 4: PCU rigid body motion at 884 Hz in the complex plane

The presented consideration reveals that the rigid body motion of the PCU is dominated by the translational movement in x-direction (direction of the drive shaft), which has the highest absolute value of the corresponding complex number in the rigid body motion vector. The rotational motions are also present in the dynamic response of the PCU but with much lower amplitudes. The absolute values of the rotation are three orders of magnitude lower than the translation.

In order to identify the most important DOF for the transmission of structure borne sound it is not sufficient to consider only the motion of the PCU. High acceleration e.g. in x-direction don't necessarily mean that this DOF is responsible for the highest amount of vibration energy that is transferred through the PCU mounts. The second important quantity that must be considered is the structural impedance of the mounting. The structural impedance is defined as $Z = F/v$, where F is the dynamic force acting on the structure and v the resulting structural velocity. This means that structures with high impedance need higher dynamic forces in order to produce the same structural velocity. Higher dynamic forces result in a higher amount of vibration energy that is fed into the structure. For the PCU this means that in order to estimate the critical DOF of the rigid body motion, which primarily induce structure borne sound, the corresponding impedance of structural mounts must be considered.

For this purpose, the structural impedance of the PCU mounts is measured using the triaxial accelerometers and an impulse hammer. Figure 5 shows the comparison of structural impedances in three coordinate directions measured on the mount 2 (see Figure 2). This mount is selected for the consideration due to the fact that mounts 1 and 2 are connected to a stiffer frame and assumed to be more important for the transmission of structure borne sound than mounts 3 and 4. In Figure 5 it can clearly be seen that, at the targeted frequency of 884 Hz, the structural impedance of the mount is similar for every direction of space. Regarding vibration amplitudes of the rigid body motion, considered in Figure 4, similar structural impedances mean that the DOF in x-direction seems to have a major importance for the structure borne sound and is therefore primarily addressed in the design of the vibration isolation system presented in the next section.

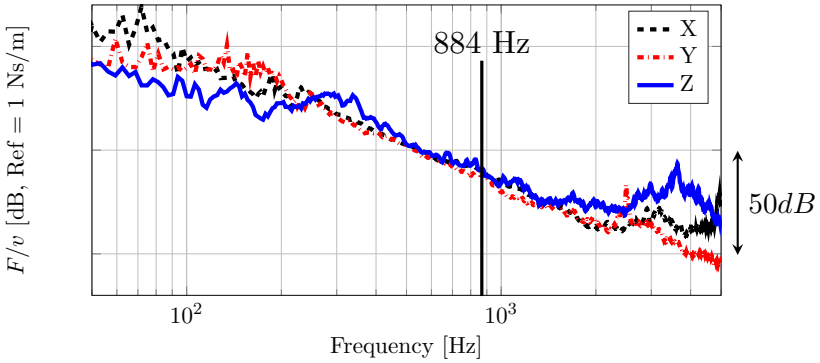

Figure 5: Measured structural impedances at mount 2

3. Design of the simplified testbed and the improved mounting

Due to the fact that neither the aircraft nor the fully equipped hydraulic setup is available for the verification of the vibration isolation system, a simplified testbed must be provided for the experimental campaign. According to the results of the previous section, the main requirement of the testbed must be the similarity regarding the rigid body motion and structural impedances of the mounting. Using the geometrical data of the PCU and the surrounding structure, a simplified dummy PCU and an aluminium basement are designed. The dummy PCU has the similar weight, centre of gravity and moments of inertia. The basement represents the stiffened aluminium structure with original PCU mounts, which have similar strcutural impedances compared to the real aircraft structure. The geometry of the dummy PCU, the designed testbed as well as the derived FE model of the testbed are shown in Figure 6.

The main idea behind the vibration isolation with the modified mounting is the reduction of the structural stiffness in the direction of the critical DOF by the simultaneous perpetuation of

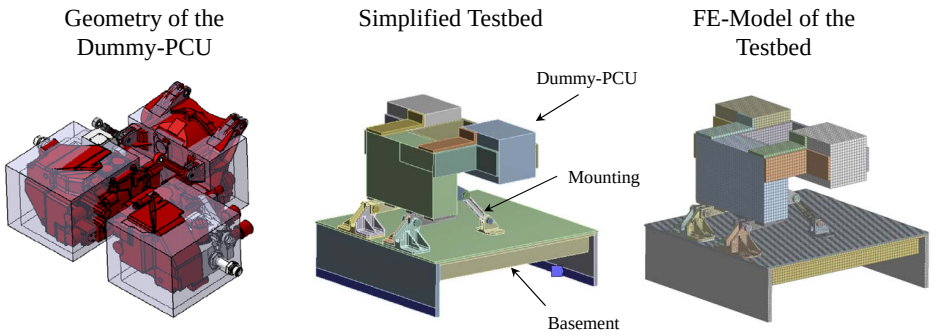

Figure 6: Design of the simplified testbed.

the capability to carry the high torque of the PCU. In order to reduce the stiffness in x-direction and still carry the required torque of $M > 1500$ Nm the modified mounting is designed. This modified mounting is similar to a cantilever spring and it is shown next to the reference mounting in Figure 7.

The design of the modified mounting also allows a simple integration of piezoceramic patch actuators as a part of the active vibration isolation system. DuraAct P-876A15 actuators with 0.5 mm thick piezoceramic layer and the operating voltage of -250 to 1000 V are used in the modified mounting. These actuators are applied on both sides of the cantilever spring and connected to clusters as it is shown in Figure 7. The clustering of actuators reduces the amount of control channels and simplifies the vibration isolation system. Nevertheless, eight actuator channels are available for control purposes and allow the actuation of all rigid body motion DOFs of the mounted PCU.

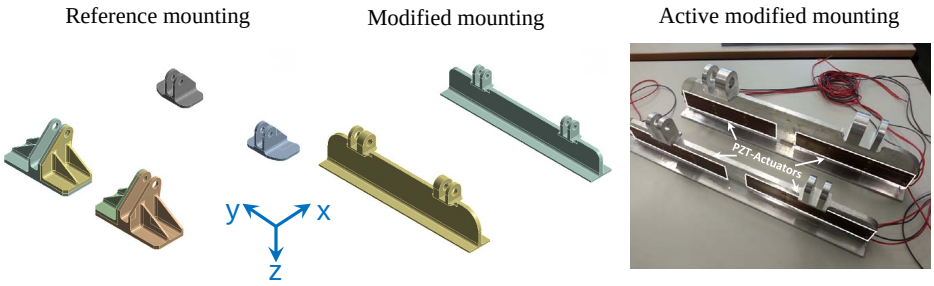

Figure 7: Reference and modified mounting

In order to demonstrate the capability of the mounting to carry the required torque the FE model, shown in Figure 6, is used for simulation. The requested amount of torque is applied at the corresponding position of the drive shaft and a numerical simulation is performed for the reference and for the modified mounting. Subsequently the strength of the mounting is analysed using the von Mises yield criterion. The results of this analysis are shown in Figure 8 for the mounting elements with highest loading. It can be noticed that the calculated safety factor of the new mounting is comparable to the reference mounting. This demonstrates the capability of the modified mounting to carry the required torque.

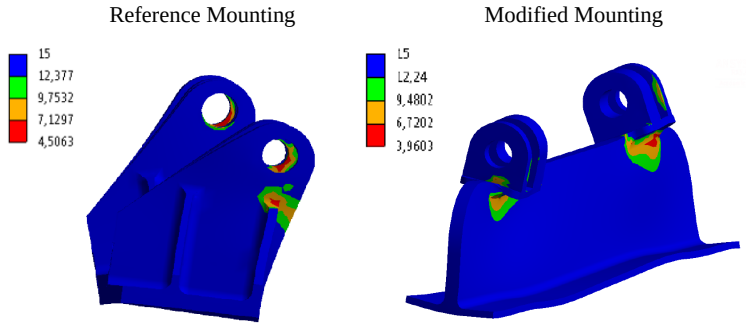

Figure 8: Safety factors of the reference and modified mounting

4. Experimental verification

4.1. Experimental setup

In this part of the paper the experimental setup is discussed, which is used for the basic demonstration of the performance of the modified mounting. In order to decouple the experimental setup from the rest of the building the testbed is installed on a suspended foundation. The dummy PCU is mounted on the basement structure either by the reference or the modified mounting. The experimental setup with reference mounting is shown in Figure 9. The excitation is provided by two RMS-SW52 shakers which are aligned in the x-direction and attached at the position of the two hydraulic motors of the real PCU. The testbed is equipped with four triaxial accelerometers located at the four attachment points of the PCU mounting. Additional accelerometers are located at the dummy PCU itself and on the structural basement. In order to measure transfer functions two force sensors are located at the shaker attachment points.

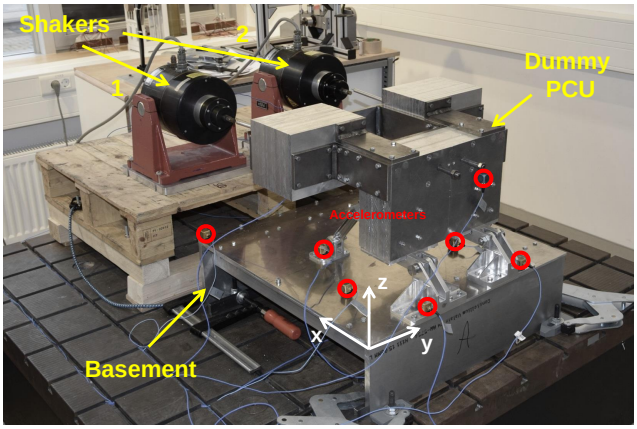

Figure 9: Experimental setup with reference mounting

4.2. Passive vibration isolation performance

In the first part of the experiments the passive vibration isolation performance of the modified mounting is analysed. For this purpose the testbed is excited by the uncorrelated, bandlimited, white noise signal and the transfer functions between the force sensors and triaxial accelerometers

at the PCU mounting are measured for the reference and the modified case. In order to allow the verification of the vibration isolation performance with a single metric, the transfer functions in x-direction from both shakers to all accelerometers are averaged and plotted in Figure 10. It can be seen that the averaged transfer function and therefore the transmitted vibration energy of the modified mounting at the targeted frequency of 884 Hz is reduced by 8 dB. The analysis of the transfer functions in y- and z-direction reveals a reduction of 4 dB and an increase of 1.5 dB respectively.

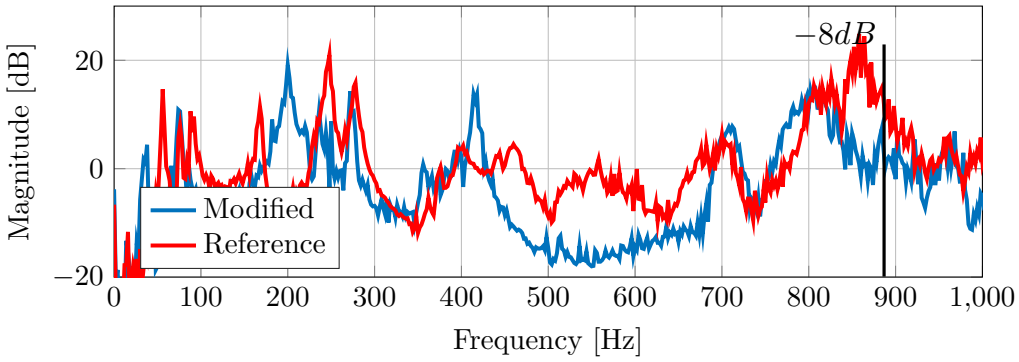

Figure 10: Averaged transfer functions of the reference and modified mounting in x-direction

4.3. Synthesis of the feed-forward controller

Reduction of multitonal disturbances is the best application scenario for an active adaptive feed-forward control system, because a coherent reference signal can easily be generated from the rotation frequencies of the hydraulic drives in the PCU [11]. Furthermore, this kind of reference signal is not disturbed by any feedback effects of the active feed-forward controller, which affect the stability of the active control system [12]. In order to evaluate the performance of the active vibration isolation system, an optimal feed-forward controller is implemented which exactly predicts the performance of an adaptive feed-forward controller in steady state [13]. In order to give a short summary of how the optimal filter is derived in the experiments a brief description of a SISO (single input single output) optimal causal feed-forward controller is given in this section. The control system which is applied to the PCU mounting is a MIMO (multiple input multiple output). The detailed information about the MIMO case can be found in [13].

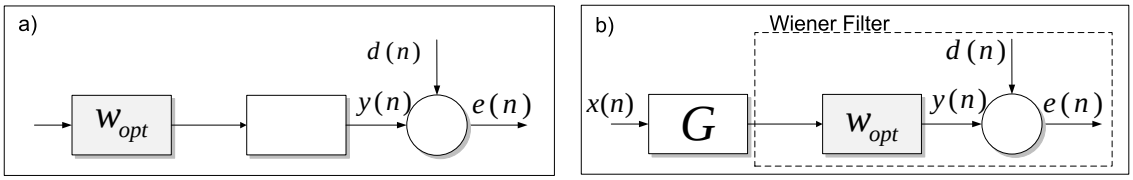

Figure 11: Block diagram of a feedforward control system for physical implementation (a) and for filter calculation (b)

A typical block diagram of a feed-forward controller is shown in Figure 11. If it is assumed that the optimal filter $\mathbf{w_{opt}}$ and the secondary path transfer function $\mathbf{G}$ are linear time-invariant systems, the order of the systems can be reversed [13]. Reversing $\mathbf{G}$ and $\mathbf{w_{opt}}$ allows the

application of the classical Wiener Filter theory by using filtered reference signals $x'(n)$. These filtered reference signals can be evaluated for the SISO case by

$$x'(n) = \sum_{r=0}^{R-1} g_r x(n-r), \tag{1}$$

in which $x(n)$ is the reference signal at the discrete time n, g_r are the coefficients of a finite impulse response (FIR) filter representing the secondary path. R is the length of the secondary path FIR filter. A quadratic cost function of the error signal is assumed as

$$J = E[e(n)^T e(n)] \tag{2}$$

in which $E[\cdot]$ is the expectation operator. Assuming that the signals are stationary and ergodic, the expectation operator can be calculated by averaging over time. Referring to Figure 11b, the Wiener Filter can be calculated by using the autocorrelation matrix $\mathbf{R_{x'x'}}$ of the filtered reference signal, the cross-correlation vector $\mathbf{r_{x'd}}$ of the filtered reference signal, and the disturbance signal $d(n)$ [13].

$$\mathbf{w_{opt}} = \mathbf{R_{x'x'}}^{-1}\mathbf{r_{x'd}}. \tag{3}$$

The filtered reference signal as a vector of length L can be formulated as follows

$$\mathbf{x'}(n) = \left[x'(n)x'(n-1)\cdots x'(n-L+1)\right], \tag{4}$$

the auto- and cross-correlation matrix of the filtered reference signal can be described by

$$\mathbf{R_{x'x'}} = E\left[\mathbf{x'^T}(n)\mathbf{x'}(n)\right] = \tag{5}$$

$$\begin{pmatrix} r_{x'x'}(0) & r_{x'x'}(1) & ... & r_{x'x'}(L-1) \\ r_{x'x'}(1) & r_{x'x'}(0) & ... & r_{x'x'}(L-2) \\ \vdots & ... & \ddots & \vdots \\ r_{x'x'}(L-1) & r_{x'x'}(L-2) & ... & r_{x'x'}(0) \end{pmatrix} \tag{6}$$

with

$$r_{x'x'}(k) = E[x'(n)x'(n-k)]. \tag{7}$$

The autocorrelation matrix is symmetric and therefore it is assumed that

$$r_{x'x'}(k) = r_{x'x'}(-k). \tag{8}$$

The crosscorrelation vector is described by

$$\mathbf{r_{x'd}} = E\left[\mathbf{x'^T}(n)d(n)\right] = \tag{9}$$

$$[r_{x'd}(0) \quad r_{x'd}(1) \quad ... \quad r_{x'd}(L-1)]^T. \tag{10}$$

The performance of the systems can be evaluated in terms of the residual error signal

$$e(n) = d(n) - \sum_{r=0}^{R-1} g_r \mathbf{w_{opt}^T}\mathbf{x}(n-r), \tag{11}$$

in which $\mathbf{x}(n)$ is the reference signal vector of length L described by

$$\mathbf{x}(n) = [x(n) \quad x(n-1) \quad ... \quad x(n-L+1)]^T. \tag{12}$$

The calculation of the optimal feed-forward controller for the experiments is subdivided in following steps:

- Experimental identification of the secondary path
- Synchronous measurement of the reference signal and the disturbance signal
- Offline calculation of the optimal filter with Equation 3
- Implementation of the filter taps into the Digital Signal Processor (DSP)

4.4. Identification of the control plant

According to equation 1 an accurate secondary path model **G** is required in order to calculate filtered reference signals. The secondary path state-space model can be identified by a multi-reference test. In this test, control actuators of the modified PCU mounting are excited by an uncorrelated bandlimited white noise and the signals at the error sensors (triaxial accelerometers at the PCU mounting) are sampled simultaneously. In order to reduce the high frequency noise and avoid aliasing effects all signals are low-pass filtered and subsequently recorded by a DSP. The corresponding experimental setup for the modified mounting is presented in Figure 12.

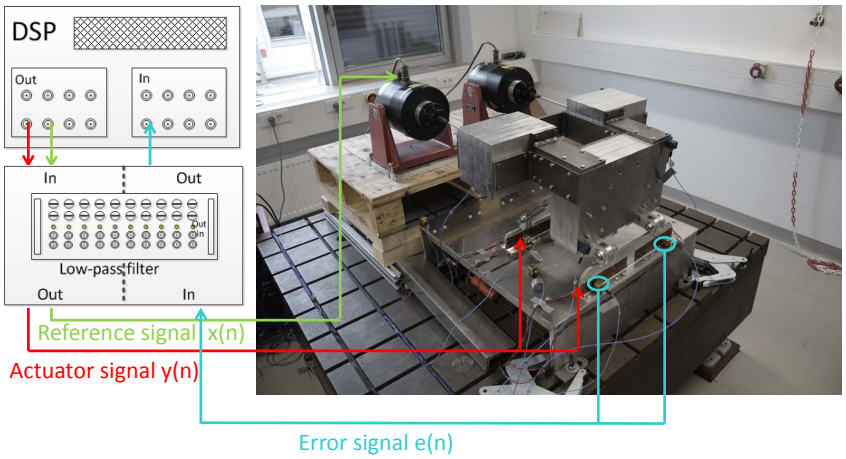

Figure 12: Experimental setup with active control system

In order to enhance the signal to noise ratio an oversampling method is used for data acquisition. Finally the measured time data is downsampled to the desired frequency of 4000 Hz and post-processed by a subspace based identification algorithm, shown in [14], in order to create state-space model of the secondary path. The accuracy of the model can be verified by the comparison of the singular values of the identified state-space model and the measured frequency response functions (FRF) in Figure 13.

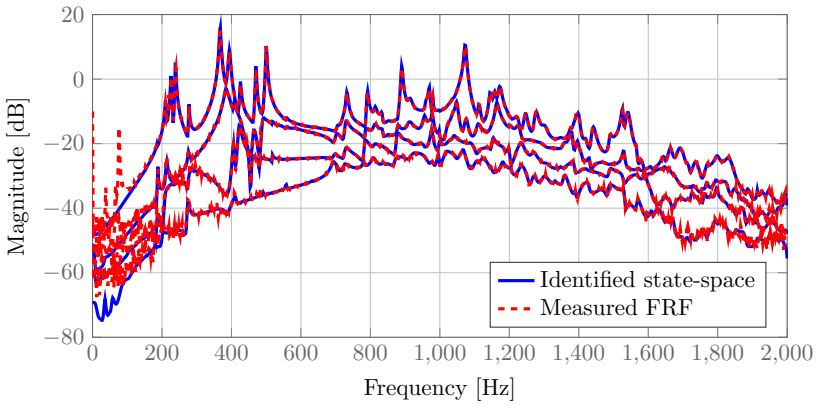

Figure 13: Singular values of the identified model and of the measured FRFs

4.5. Performance of the active vibration isolation system

In this section the results of the applied control systems are presented. Two different MIMO control systems are investigated on the simplified PCU demonstrator. The first control system

addresses only the fundamental frequency of 884 Hz and the x-direction of motion and includes four input and four output channels. The actuators are clustered to four channels, each cluster addresses one of the opposite sides of the modified mounting. Four accelerometer channels in x-direction, located at the basement of the mounting, are used as error sensors. The second system uses the same actuator configuration but addresses two frequencies of 884 and 1768 Hz and sensor channels x- and z-direction.

The disturbance of the PCU demonstrator is provided by a tonal excitation of the corresponding frequencies using the installed shakers. The preliminary analysis of the structural response to this excitation reveals a high content of higher harmonics, which indicates a high amount of non-linearities in the PCU demonstrator. For this structural response the total harmonic distortion is calculated and it shows values of up to 0.4 on different accelerometer channels. This high amount of non-linearities can be explained by the differential construction of the demonstrator, which includes many parts and joints. Therefore bearing play and non-linear stiffnesses are unavoidable.

Due to the explained non-linearities the identificated linear state-space or FRF models are only valid for a small amplitude range of excitation. The amplitudes per frequency at the accelerometers during the identification process are rather small compared to the sinusoidal disturbances of the PCU. This is caused by the energy spread to a wide frequency band by using a bandlimited white noise signal for the identification of the models. Thus, the amplitude of the sinusoidal disturbance applied during the experiments has to be matched to the amplitudes which is used during the identification process. In further investigations only the transfer functions at the specified frequencies can be measured and by that the amplitudes can be matched to real working conditions. In the presented study only small disturbance amplitudes are applied to the PCU. Nevertheless, the control voltage applied to the actuators are far below 100 V and there for larger disturbances can be controlled in further experiments.

Therefore the amplitude of the tonal disturbance during the operation of the control system is reduced in order to match the amplitude which was used in system identification procedure. The performance of the active vibration isolation system excited by the adjusted disturbance amplitudes is presented in Table 1 for two control concepts.

Controller/Frequency	**884 Hz**	**1768 Hz**
x-direction	-14.3 dB	not controlled
x- and z-direction	-10.2 dB	-8.1 dB

Table 1: Reduction of the feed-forward controllers

The first active vibration isolation system, which addresses the fundamental frequency and x-direction, shows an averaged accelerometer amplitude reduction of 14.3 dB on the basement of the mounting. The second active system, which includes additional frequency and the z-direction, shows slightly lower maximum reduction performance but still achieves an averaged values of 10.2 dB at 884 Hz and 8.1 dB at 1768 Hz respectively.

5. Conclusions

The presented paper investigates the vibration isolation of hydraulic drives, exemplarilly demonstrated at the PCU. Main focus of the paper is set to the modification of the PCU mounting under the requirements of reduced vibration transmission, load bearing capability and the integration of active elements.

The analysis of the dynamic response of the PCU reveals the critical frequency of 884 Hz and DOFs of the rigid body motion in x-direction, which must be addressed by the vibration isolation system in order to reduce the noise levels in the passenger cabin. Based on this analysis

the modified mounting is designed. This mounting is similar to a cantilever spring and it reduces the structural stiffness in the direction of the critical DOFs in x-direction. As requested, it is capable to carry high reaction torques of the hydraulic drive.

The experimental verification of the vibration isolation performance is conducted on a simplified demonstrator, which has been designed to reproduce the basic structural dynamic behaviour of the PCU, mounting and the surrounding structure. The comparison of the reference and modified mounting regarding vibration isolation performance reveals an improvement of the modified mounting by 8 dB in the addressed direction of the rigid body motion.

In addition to the modified mounting, two active control systems are implemented in order to furtherly improve the performance of the vibration isolation. The first feed-forward control system shows a maximum reduction of the transmitted vibrations of 14.3 dB. The second system improves the isolation performance on the second frequency of 1768 Hz and an additional DOF in z-direction and shows a reduction of up to 10.1 dB. In combination of the passive modified mounting and the active vibration isolation system a total vibration amplitude reduction of approximately 18 dB at 884 Hz is demonstrated.

The main challenge in the implementation of the active control system is the high amount of structural non-linearities of the experimental demonstrator. These effects must be taken into account during the system identification procedure and the operation of the active control system. This means that the feed-forward controller must be designed using the state-space model, which is identified with excitation amplitudes that are close to the operational conditions on the PCU.

In order to increase the technology readiness levels, the modified mounting must be integrated in the real operating environment. The analysis of non-linearities and the feasibility and robustness of the designed feed-forward controller must be evaluated under real operational amplitudes.

References

[1] Martin Recksiek. Advanced high lift system architecture with distributed electrical flap actuation. In *Proceedings of the 2nd International Workshop on Aircraft System Technologies*, pages 49–59, 2009.
[2] Yulin Wu, Shengcai Li, Shuhong Liu, Hua-Shu Dou, and Zhongdong Qian. *Vibration of hydraulic machinery*. Springer, 2013.
[3] Stan Skaistis. *Noise control for hydraulic machinery*, volume 8. CRC Press, 1988.
[4] Henning Strüber. The aerodynamic design of the a350 xwb-900 high lift system. In *29th international congress of the aeronautical sciences*, 2014.
[5] Eugene I Rivin, Eugene I Rivin, and Eugene I Rivin. *Passive vibration isolation*. Asme press New York, 2003.
[6] Kazuto Seto, Katsumi Sawatari, Akio Nagamatsu, Masao Ishihama, and Kazuhiro Doi. Optimum design method for hydraulic engine mounts. Technical report, SAE Technical Paper, 1991.
[7] Joong Jae Kim and Heon Young Kim. Shape design of an engine mount by a method of parameter optimization. *Computers & structures*, 65(5):725–731, 1997.
[8] Tie-jun Yang, Xin-yu Zhang, You-hong Xiao, Jin-e Huang, and Zhi-gang Liu. Adaptive vibration isolation system for diesel engine. *Journal of Marine Science and application*, 3(2):30–35, 2004.
[9] BT Kletz, J Melcher, and M Sinapius. Active vibration isolation of rear-view mirrors based on piezoceramic double spiralactuators. *Proceedings of ISMA2012-USD2012*, pages 305–320, 2012.
[10] Franz Holzweißig and Hans Dresig. *Lehrbuch der Maschinendynamik: maschinendynamische Probleme und ihre praktische Lösung*. Springer-Verlag, 2013.
[11] Thomas Haase, Malte Misol, and Michael Rose. Optimal placement of flat piezoceramic actuators for feedforward systems under the influence of real-time hardware delays. *Journal of Sound and Vibration*, 345:34–46, 2015.
[12] Sen M. Kuo and Dennis R. Morgan. *Active noise control system: algorithms and DSP implementations*. John Wiley & Sons, INC., 1.aufl. edition, 1996.
[13] Stephen Elliott. *Signal processing for active control*. Academic Press, 1.aufl. edition, 2001.
[14] Tohru Katayama. *Subspace methods for system identification*. Springer Science & Business Media, 2006.